End-Wall Heat-Transfer Effects on the Trajectory of a Reflected Shock Wave

BRADFORD STURTEVANT AND ERIK SLACHMUYLDERS*
Graduate Aeronautical Laboratories, California Institute of Technology, Pasadena, California
(Received 30 October 1963)

The trajectory of a reflected shock wave has been measured near the end wall where the motion is perturbed by the displacement effect of heat transfer to the wall. In this experiment an x, t diagram of the reflection of an $M_s = 4.08$ shock wave was constructed by measuring shock arrival times with small probes. The parameter that measures the (negative) displacement thickness of the end-wall thermal layer, a "Reynolds number" R based on the shock velocity, the time after reflection, and the thermal diffusivity was varied between 9 and 600. In this range the measured deviation of the shock trajectory from ideal varied from $1\frac{1}{2}$ to 17 shock thicknesses. The shock velocity was determined by differentiating a least-squares fit of the data to a fourth-order polynomial in $R^{-\frac{1}{4}}$. In the range of the experiments the shock accelerated from a velocity that was 20% below ideal to one that was within 4% of ideal. Experiment agrees with boundary-layer theory above $R = 150$ for the shock trajectory and above $R = 25$ for the shock velocity, and implies that the exponent of the power-law dependence of the thermal conductivity on temperature is 0.81 ± 0.02. The small deviation of the shock velocity from boundary-layer theory predicted for $R < 100$ by higher-order theory is not observed, though since this theory falls just within the estimated experimental error this result is somewhat qualified. In any case, the unexpected agreement with first-order theory at small R indicates that molecular effects, such as temperature jump, do not play a large role when the shock is more than ten shock thicknesses from the end wall.

I. INTRODUCTION

AFTER a strong normal shock wave reflects from a plane heat-conducting wall (Fig. 1) the shock-heated gas adjacent to the wall is cooled by heat transfer. The gas in the growing thermal layer is relatively dense, and in order to supply the required mass a displacement velocity toward the wall is induced in the hot gas far away. This flow perturbs the trajectory of the reflected shock wave. Since the shock does not quite stagnate the gas as it would in the ideal non-heat-conducting case, the velocity jump across the shock is less, so the shock is weaker. The magnitude of the displacement velocity is measured by a Reynolds number[1] based on the time t after shock wave reflection, $R = u_R^2 t/\kappa_5$, where u_R is the velocity of the shock wave in laboratory coordinates and κ_5 is the thermal diffusivity of the gas behind the reflected shock wave. For times sufficiently large that $R^{-\frac{1}{4}} \ll 1$ the thickness of the thermal layer, which grows as $t^{\frac{1}{2}}$, is small compared to the distance $u_R t$ that the shock has traveled, and boundary-layer theory can be used to calculate the displacement velocity. This velocity serves as the wall boundary condition in the (linearized) calculation of the outer inviscid flow, with the result that the deviation of the shock trajectory from ideal is predicted to grow as $t^{\frac{1}{2}}$.

At small times, when the displacement velocity is large, it is expected that higher approximations to boundary-layer theory will be necessary. A second-order correction to the shock velocity can be obtained by improving the calculation of the outer flow, for a consequence of matching the inner and outer flows is that the displacement velocity calculated from first-order boundary-layer theory is also the wall boundary condition for the second-order inviscid theory. However, the correction to the shock position can not be calculated from this theory because the second-order velocity is not integrable. Ultimately it should be necessary to account for strong interaction between inner and outer flows.

At even smaller times the shock thickness is no longer negligible, and a theory for the reflection of a thick shock wave, possibly even including molecular effects such as thermal accommodation, should be necessary for predicting the shock trajectory. The reflection of very weak shocks has been treated by Watts[2] but there is no theory available for strong shocks, either using the Navier–Stokes equations or kinetic theory.

* Present address: European Space Research Organization, Delft, Holland.

[1] Actually a Péclet number, but in the light of the analogy with viscous boundary layers discussed below we prefer "Reynolds number."

[2] A. M. Watts, private communication; based on the theory of the leading edge of a shock-induced boundary layer worked out independently by A. M. Watts, Ph.D. thesis, University of Sydney (1961); and M. Sichel, Phys. Fluids **5**, 1168 (1962).

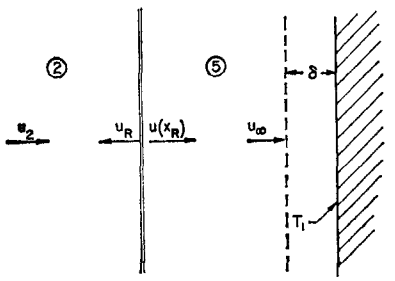

FIG. 1. Schematic of reflecting shock wave and end-wall thermal layer.

This problem is analogous to that of steady supersonic flow over a wedge, in which the shock shape is perturbed by the displacement effect of the velocity boundary layer.[3] However, the displacement thickness on the wedge is positive, tending to strengthen the shock, while in our shock-tube problem it is negative and weakens the shock. In both cases higher approximations predict a dimunition of the displacement effect, i.e., a tendency to smooth out the leading-edge singularity. For example, the strong interaction near the leading edge of a wedge in steady flow thins the boundary layer (e.g., in hypersonic flow $\delta \sim x^{\frac{3}{4}}$). Another difference, due to the fact that there are no large velocities in the shock-tube problem, is that viscosity plays no role there, resulting in a fundamental simplification of the boundary-layer equations.

Apparently, the only experiments demonstrating boundary-layer effects on the shape of a shock wave on a wedge are those of Chuan,[4] but excessive scatter in his results precludes quantitative conclusions. The special case of a flat plate aligned parallel to the free stream has been studied more extensively. For example, Kendall[5] has shown that the shock shape at $M = 5.8$ agrees with that calculated from the Friedrichs theory, and Cheng, *et al.*,[6] have correlated their measurements of shock shape at $M = 12$ with a hypersonic strong-interaction theory.

In this paper we report measurements of the trajectory of a reflected shock wave over a range of Reynolds numbers ($600 > R > 9$) within which the deviation from ideal varies from 8% to 45%. Our experiments indicate that the shock trajectory is predicted accurately ($\pm 2\%$) by first-order boundary-layer theory[7] for $R > 150$. At $R = 150$ the deviation from ideal is 15%. The shock *velocity* implied by our measurements agrees within 1% with boundary-layer theory down to $R = 25$ where the deviation from ideal is 20%. *At $R = 25$ the shock wave is less than ten shock thicknesses from the wall.* In fact, *both* the boundary-layer theory and the higher approximation fall within the experimental scatter of $\pm 2\%$ down to $R = 25$, the theoretical correction for low Reynolds number effects being small in this problem. Thus, for the purpose of shock-tube studies in the reflected-shock region, perturbations due to the end-wall thermal layer can be computed very accurately using boundary-layer theory.

Our experiments were made in the 17-in. shock tube of the Graduate Aeronautical Laboratories at the California Institute of Technology[8] using new thin-film-covered Pyrex filament heat-transfer gauges[9] to detect the passage of the shock wave. Signals recorded simultaneously from two or three filament gauges at different distances from the end wall defined the time of reflection ($t = 0$) by extrapolation of the trajectory of the incident shock wave and gave two or three points on the x, t diagram of the reflected wave. Seventy-nine points were obtained from thirty-four runs in argon at the same incident shock Mach number ($M_s = 4.08 \pm 0.10$) but at various pressures ($p_1 = 50$, 100, and 500 μ Hg) and probe locations ($0.10 < x < 0.95$ in.).

II. BOUNDARY LAYER THEORY

Application of the Howarth transformation to the equations for a constant-pressure thermal layer in a perfect monatomic gas with heat conductivity proportional to temperature results in the classical heat equation for the temperature. Consequently, with the boundary conditions of this problem, the temperature profile is a complementary error function in the stretched boundary-layer variable $\eta = \xi/(4\kappa_5 t)^{\frac{1}{2}}$, where $d\xi = (\rho/\rho_5)\,dx$ and $\kappa_5 = k_5/c_p\rho_5$. The displacement velocity, u_∞, is found by integrating the continuity equation in the usual manner using the known density profile ($\rho/\rho_5 = T_5/T$),

$$u_\infty = -(1 - T_1/T_5)(\kappa_5/\pi t)^{\frac{1}{2}}. \qquad (1)$$

T_1, the initial temperature, is used here as the wall temperature because in practice the difference is negligible. Equation (1) is the boundary condition at $x = 0$ for the computation of the external flow field: When boundary-layer theory is valid, perturbations in the external flow are so small that

[3] L. Lees, J. Aero. Sci. **20**, 794 (1953).
[4] R. L. Chuan, Ph.D. thesis, California Institute of Technology (1953).
[5] J. M. Kendall, Jr., J. Aero. Sci. **24**, 47 (1957).
[6] H. K. Cheng, J. G. Hall, T. C. Golian, and A. Hertzberg, J. Aerospace Sci. **28**, 353 (1961).
[7] F. A. Goldsworthy, J. Fluid Mech. **5**, 164 (1958).
[8] H. W. Liepmann, A. Roshko, D. Coles, and B. Sturtevant. Rev. Sci. Instr. **33**, 625 (1962).
[9] E. Slachmuylders, A.E. thesis, California Institute of Technology (1963).

linearization is possible, so the velocity just behind the shock (assuming the shock to be in its unperturbed position, $x_R = u_R t$) is[10]

$$u(x_R) = -\left(1 - \frac{T_1}{T_5}\right)\left[\frac{\kappa_5}{\pi t\left(1 - \frac{u_R}{a_5}\right)}\right]^{\frac{1}{2}}, \qquad (2)$$

where u_R is computed in terms of the incident-shock Mach number, $M_s = u_s/a_1$, using ideal shock-tube theory,

$$\frac{u_R}{a_1} = \frac{1 + 2[(\gamma - 1)/(\gamma + 1)](M_s^2 - 1)}{M_s}. \qquad (3)$$

Now, the small change in shock velocity Δu_R induced by $u(x_R)$ is given by the shock jump conditions, e.g.,

$$\frac{\Delta u_R}{u(x_R)} = \left(\frac{4}{\gamma + 1} - \frac{M_s^2 - 1}{\gamma M_s^2 - \frac{1}{2}(\gamma - 1)}\right)^{-1}. \qquad (4)$$

Finally, the correction to the trajectory of the reflected shock wave is computed by integrating the velocity decrement [Eqs. (2) and (4)]. The fractional deviation from the ideal trajectory is

$$(x_R - u_R t)/u_R t = -f(M_s, \gamma)(\kappa_5/u_R^2 t)^{\frac{1}{2}}, \qquad (5)$$

where

$$f = \frac{2}{\pi^{\frac{1}{2}}} \frac{1 - T_1/T_5}{(1 - u_R/a_5)^{\frac{1}{2}}} \left(\frac{4}{\gamma + 1} - \frac{M_s^2 - 1}{\gamma M_s^2 - \frac{1}{2}(\gamma - 1)}\right)^{-1},$$

or, defining the nondimensional shock position $X = u_R x_R/\kappa_5$,

$$(R - X)/R = f/R^{\frac{1}{2}}. \qquad (6)$$

The ratio of the actual shock velocity to the ideal, $(dx_R/dt)/u_R$, is

$$dX/dR = 1 - f/2R^{\frac{1}{2}}. \qquad (7)$$

The characteristic length κ_5/u_R is of the same order as the mean free path ahead of the reflected wave; in our experiments $\kappa_5/u_R \doteq 1.3\Lambda_2$. For moderately strong shocks the function f is nearly independent of shock strength, being 1.773 for $M_s = 4.08$ and approaching, as $M_s \to \infty$, the value 1.93 (for $\gamma = \frac{5}{3}$). The nondimensional x, t diagram predicted by Eq. (6) for $M_s = 4.08$ is shown in Fig. 2.

The assumption that heat conductivity is proportional to temperature is not a good representation of the actual behavior of argon. The more general assumption that the conductivity is proportional to some power of the temperature, say

$$k \sim T^{\omega}, \qquad (8)$$

is much better because a simple power-law intermolecular potential energy function [which implies Eq. (8)] is quite adequate for describing particle interactions at high temperatures.[11] Actually, available data[12] indicate that in the temperature range found in the end-wall thermal layer at $M = 4.1$ ($296° < T < 4000°$K) ω is about 0.81 at both limits but drops to a minimum of less than 0.70 at about 1000°K. If Eq. (8) is used in the above boundary-layer theory, f becomes a function of ω, i.e., $f(M_s, \gamma, \omega)$, and analytical solutions cannot be obtained. However, several numerically computed values of f at the conditions of our experiments ($T_5/T_1 = 13.0$) but for different ω's have been generously supplied to us by D. J. Collins of the Jet Propulsion Laboratory. If we determine the actual value of f from our measurements, then these numerical results can be used to determine ω. This is done in Sec. V, with the result that $\omega = 0.81 \pm 0.02$. Note that because of the weak dependence of f on Mach number for moderately strong shocks this experiment is particularly suitable for a detailed study of the accuracy of Eq. (8) over a large range of temperatures and for a variety of gases. However, this was not the purpose of the present work which was carried out in argon at $T_5 = 4000°$K only.

III. HIGHER APPROXIMATIONS

Since in our experiments the shock wave is detected when it is as little as three shock thicknesses from the end wall, it is of some interest to inquire into the deviations from boundary-layer theory at low Reynolds numbers predicted by higher approximations. The efforts that have been made along this line with steady flow problems have been reviewed by Van Dyke and others.[13] In this section we will discuss higher approximations to the trajectory of a reflected shock wave.

An approximate higher-order weak-interaction

[10] F. A. Goldsworthy, in Ref. 7, integrates the inviscid equations along both sets of characteristics, taking into account the reflection of perturbations from the shock wave. However, the reflection coefficient is well known to be very small [cf. M. J. Lighthill, *Higher Approximations in Aerodynamic Theory* (Princeton University Press, Princeton, New Jersey, 1960), p. 63], so it is consistent with the linearization to make the present simpler calculation. Neglecting reflections changes $u(x_R)$ by only $1\frac{1}{2}\%$ in the present case.

[11] I. Amdur and E. A. Mason, Phys. Fluids **1**, 370 (1958).

[12] Reference 11, p. 378; and J. O. Hirschfelder, C. F. Curtiss, and R. B. Bird, *Molecular Theory of Gases and Liquids* (John Wiley & Sons, Inc., New York, 1954), p. 573.

[13] M. D. Van Dyke, Lockheed Missiles and Space Division Rept. No. LMSD-703097 (1960); W. D. Hayes and R. F. Probstein, *Hypersonic Flow Theory* (Academic Press, Inc., New York, 1959), Chap. 9.

theory can be formulated by neglecting the reflection of disturbances from the shock wave. Then the behavior of the boundary layer can be abstracted directly from Traugott's analysis of the impulsive motion of a plate with heat transfer[14] by setting the plate velocity equal to zero. For example, the second-order correction to the displacement velocity, u_∞, is given by Eq. (22) of Ref. 14,

$$\Delta u_\infty = -\frac{\eta}{\pi^{\frac{1}{2}}}\left(1 - \frac{T_1}{T_5}\right)\frac{\kappa_5}{a_5 t}. \tag{9}$$

As shown by Van Dyke,[15] the second approximation to the *outer* flow results from a second-order inviscid calculation, but, as a consequence of the matching procedure, the boundary condition is still the *first* approximation to the displacement velocity [Eq. (1)]. The higher-order correction to the shock velocity is therefore obtained by accounting for (a) the difference between the characteristic direction used in the linear theory ($dx/dt = a_5$) and one that includes the effect of the displacement velocity, and (b) the fact that a better approximation to the shock position is given by Eq. (5). If reflections from the shock wave are neglected, the flow between the shock and the wall is a simple wave and $dx/dt = \frac{1}{2}(\gamma + 1)\, u_\infty + a_5$. The additional term decreases the characteristic speed. The effect of both (a) and (b) above is illustrated in Fig. 2 where first- and second-order characteristics carrying disturbances to the shock at the same time are compared. Since the perturbation on the second-order characteristic originates later, it is smaller. Thus, second-order theory predicts a dimunition of the displacement effect. The velocity calculated neglecting reflections from the shock (a sort of shock-expansion theory) is plotted in Fig. 7. Being correct to at least second order, it can be represented analytically as

$$\Delta u_R/u_R = -f_1/R^{\frac{1}{2}} + f_2/R. \tag{10}$$

In the previous section we integrated the first term to get the first-order shock position, but the same procedure is not possible here because the integral of the second term is singular at $R = 0$. This situation is analogous to that encountered in integrating the skin friction on a flat plate in low speed flow,[13] where the third-order term is not integrable.

The effect of the outer flow on the boundary layer (strong interaction) can be estimated by assuming that the displacement velocity depends on *local* external conditions, c.f. Eq. (1),

$$u_\infty = -\text{const}\,(1 - T_1/T_\infty)(\kappa_\infty/t)^{\frac{1}{2}}. \tag{11}$$

The temperature, which is lower than ideal, tends to decrease κ_∞ while the density, which is also lower, tends to increase it. If the reflected shock were strong the temperature effect would dominate and the boundary layer would be thinner, but actually the strength of reflected shock waves is limited. In fact, in a perfect gas the upper limit on the Mach number of the shock relative to the gas ahead of it, $M_R = (u_R + u_2)/a_2$, is only $[2\gamma/(\gamma - 1)]^{\frac{1}{2}} = 5^{\frac{1}{2}}$. At the conditions of our experiment the temperature and density effects almost exactly cancel; *there is no strong interaction.*

At low enough R the effects of rarefaction, such as thermal accommodation and possibly even gaseous adsorption, must be accounted for. Temperature jump can be accounted for in the continuum theory by replacing the boundary condition $T = T_1$ at $x = 0$ with the slip boundary condition $T - T_1 = \Lambda\, \partial T/\partial x$. However, since the thermal layer generated by a strong reflecting shock wave is so dense, the mean free path at the wall tends to be very small. In fact, the effect of this change on the boundary- layer theory is negligible for our experiments.

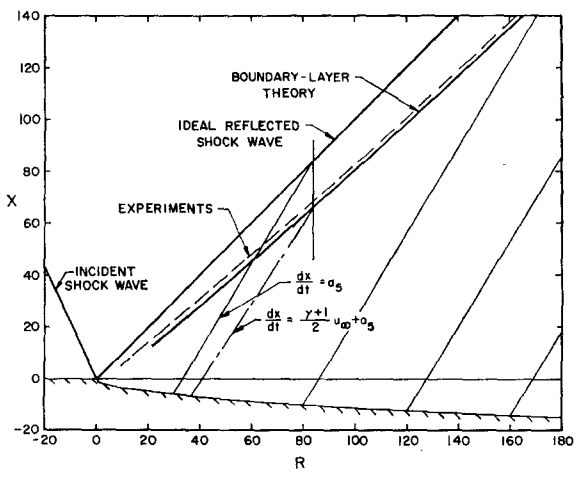

FIG. 2. Nondimensional x, t diagram of the reflecting shock wave.

IV. EXPERIMENTS

The measurement of shock trajectory in unsteady flow is in principle straightforward and accurate, requiring only the detection and timing of the wave and involving no gauge calibrations. The major problem encountered in experiments demonstrating boundary-layer effects is in detecting the shock with sufficient sensitivity at the relatively low pressures used. The device we used is a small free-molecular

[14] S. C. Traugott, J. Fluid Mech. **13**, 400 (1962).
[15] M. D. Van Dyke, Z. Angew. Math. Phys. **3**, 343 (1952).

heat-transfer gauge which is a cross between a standard thin-film heat-transfer gauge and an unheated wire. The sensitive element is a thin platinum film evaporated onto a Pyrex filament of approximately 0.005-in. diam. Filaments about $\frac{3}{4}$-in. long are mounted parallel to the end wall on 0.025-in. diam needles (Fig. 3). The resistance of a typical film is about 400 Ω which implies a film thickness of roughly 200 Å. The distance between the filament and the end wall is measured with an accuracy of better than 0.001 in. with an optical comparator. The details of probe construction are given in Ref. 9.

The reasons for using this type of gauge rather than a cold wire[16] are twofold. First, due to the nature of the output the shock can be more accurately timed, for, whereas the cold wire output is a straight line at small times, the film-coated filament, being essentially a stagnation point gauge, gives a parabolic output. The resulting large slopes and signals at small times are particularly important when, as in some of our experiments, the rise of the signal is limited by the finite thickness of the shock. In fact, Slachmuylders[9] has shown that, because of the nature of its output, the film-coated filament offers some advantages over the cold wire for measurements of the structure of moving shock waves. Second, the gauge is rugged and lasts for many runs, while wires small enough to give sufficient signal have to be replaced after every run.

In each run two or three probes are mounted on, and 3 in. from, the center-line of the shock tube. The fact that the nearest probe is 5 in. from the side wall insures that the experiments simulate reflection from an *infinite* end wall free of the effects of the side-wall boundary layer; before a disturbance

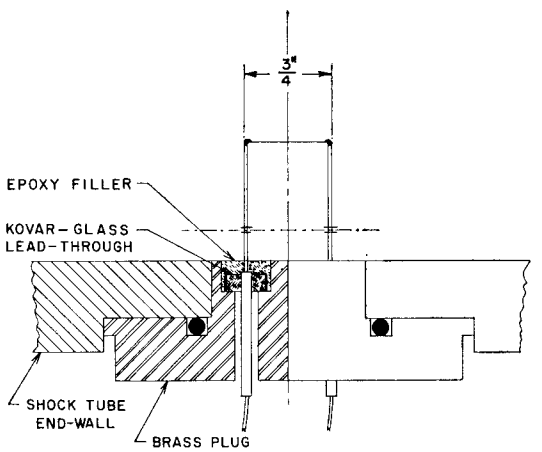

FIG. 3. Heat-transfer probe construction.

[16] W. H. Christiansen, Phys. Fluids **3**, 1027 (1960).

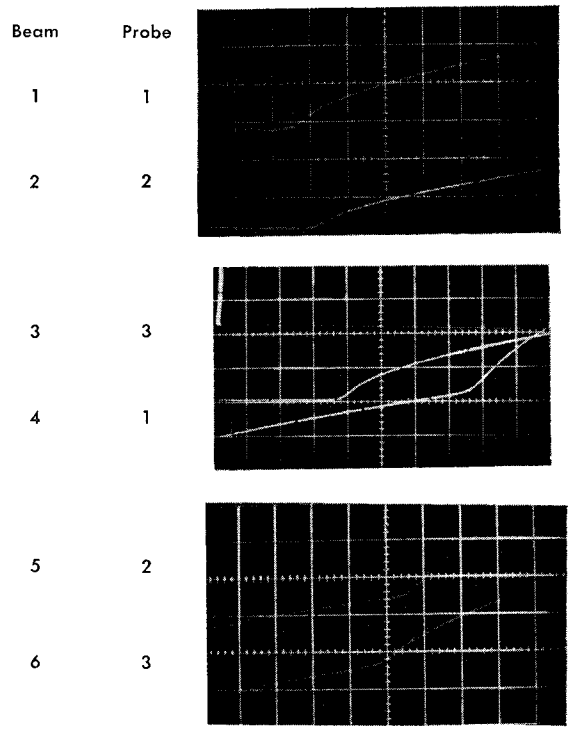

FIG. 4. Typical heat-transfer gauge traces at $p_1 = 50\mu$ Hg, $M_s = 4.12$, sweep speed = 5μ sec/cm, vertical deflection = 2 mV/cm.

can propagate from the corner at the side wall to the nearest probe the reflected shock will have traveled 3 in., more than 2 in. beyond the limit of our measurements.

Figure 4 illustrates signals of three probes recorded simultaneously during a run at $p_1 = 50\ \mu$ Hg. The signal from each probe is recorded on two traces (displaying incident and reflected shocks, respectively) in order to increase the accuracy of timing. As indicated in the figure, the shock is defined as the intersection of the line of maximum slope with the zero line. The traces, which are delayed relative to one another, are coordinated by using the timing pips in each picture.

The effects of nonuniformities due to attenuation of the incident shock wave are negligible in these experiments, the measured attenuation being only about 0.1% per foot. Similarly, shock curvature is small and its effects are thought to be negligible.

At $p_1 = 50\ \mu$ Hg the incident wave is about 0.07-in. thick and the reflected wave about 0.04-in. thick. The viscous length κ_5/u_R is about 0.015 in. The strength of the reflected wave is $M_R = 2.95$, its speed is $u_R = 0.71$ mm/μsec, and the parameter defining the "Mach angle" is $u_R/a_5 = 0.601$. In these tests the Reynolds number per cm, u_R/κ_5, varies from about 25 to 250.

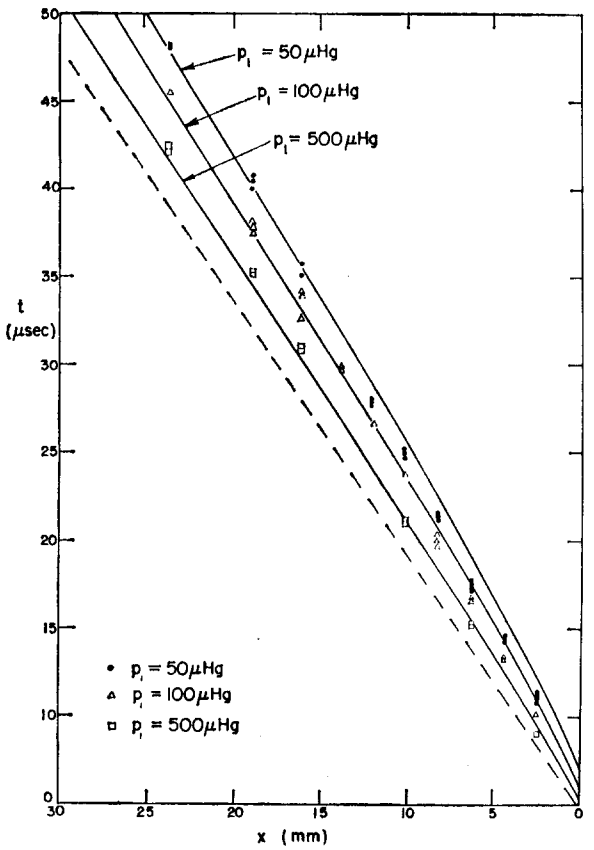

FIG. 5. Experimental results.

V. RESULTS

The results of our measurements are plotted in Fig. 5. It can be seen that the agreement with boundary-layer theory is good at large times, but that at small times the experimental points are low, particularly at low pressures. To demonstrate that the results scale with pressure as predicted by theory they can be nondimensionalized to the variables X and R. However, in doing so special attention must be paid to the behavior of κ with temperature: κ_5 is given by

$$\kappa_5 = \kappa_1(T_5/T_1)^{\omega}(\rho_1/\rho_5), \tag{12}$$

where κ_1, the value at room temperature, is well known,[17] i.e., $\kappa_1 = 3092$ cm^2/sec at $p_1 = 50$ μ Hg and $T_1 = 296$°K. κ_5 and therefore the nondimensionalization depends on ω. The appropriate value of ω is determined as follows: If the experimental results are represented by $(R - X)/R = gR^{-\frac{1}{3}}$ [cf. Eq. (6)], then because R is a function of ω, g must be also. By requiring that $g(\omega)$ as determined by the experiments equal the numerically calculated value of $f(M_s, \gamma, \omega)$ in Eq. (6), consistent values of g and ω can be obtained. We determined g from our experiments by fitting the seventy-nine data points to a fourth order polynomial in $R^{-\frac{1}{3}}$ using a least squares fit, with the result

$$\frac{R - X}{R} = \frac{1.98}{R^{\frac{1}{3}}} - \frac{0.994}{R} - \frac{21.73}{R^{\frac{4}{3}}} + \frac{55.53}{R^2} \pm 0.02. \tag{13}$$

The value $g(\omega) = 1.98$ implies[18] $\omega = 0.81 \pm 0.02$. Figure 6 is a plot of the fractional deviation of the shock trajectory from ideal vs time, nondimensionalized using this result. The first term of Eq. (13), $(R - X)/R = 1.98\ R^{-\frac{1}{3}}$, is the prediction of boundary-layer theory for $\omega = 0.81$ and is also plotted in Fig. 6, as is Eq. (13).

The $\pm 2\%$ rms deviation in Eq. (13) is essentially the same as the experimental scatter. The high quality of the data is due to the precise repeatability of conditions in our shock tube which in turn is largely due to the knife blades that are used for controlling diaphragm rupture.[8] The repeatability of Mach number has a two-fold effect; not only is the scatter in temperature, etc., reduced but also accurate determination of delay times for triggering and therefore faster sweep speeds are possible, permitting more accurate timing.

The value $\omega = 0.81$ is nearly that calculated from Refs. 12 for room temperature and from about 2500° to 4000°K, i.e., at the wall and in the outer half of the thermal layer, but somewhat larger than in the intermediate region. If the experiments can be thought of as measuring an effective or average

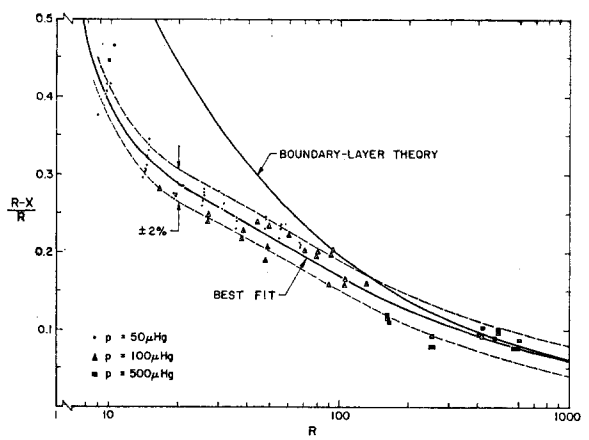

FIG. 6. Fractional deviation of shock trajectory from ideal.

[17] "Tables of the Thermal Properties of Gases," Natl. Bur. Std. (U. S.) Circ. No. 564 (1953).

[18] The estimate of error for ω was obtained by calculating the *percentage* rms deviation of Eq. (13) ($\pm 1\%$) and applying it to $g(\omega)$.

ω appropriate for describing the displacement effect of the thermal layer on the outer flow, then it can be tentatively concluded that the average is weighted toward the value of ω in the outer part of the layer.

The ratio of the actual shock velocity to the ideal value, dX/dR, implied by our measurements can be obtained by differentiating Eq. (13). This is compared in Fig. 7 with the predictions of Secs. II and III.[19] The measured velocity agrees with boundary-layer theory to much lower Reynolds numbers than the shock trajectory does, implying that the disagreement in the latter case is due to a nearly constant displacement of the shock wave from its theoretically calculated location (cf. also Fig. 2). The order of the term representing this displacement in an expansion of the shock trajectory in powers of $R^{-\frac{1}{2}}$ is of course the same as that which was unobtainable by integration of Eq. (10).

A more precise and detailed experiment than ours would be necessary to empirically evaluate these higher-order terms, however, because in the range of R where these terms are important the shock thickness becomes comparable to the deviation of the shock trajectory from ideal (in the range $9 < R < 600$ the measured deviation from ideal varies from about $1\frac{1}{2}$ to 17 shock thicknesses). Under these conditions our definition of the shock location (Fig. 4) is ambiguous and, e.g., a measurement of the entire flow field would be required for quantitative results.

We have shown that experiment agrees with boundary-layer theory above $R = 150$ for the shock trajectory and above $R = 25$ for the shock velocity, and implies that the exponent of the power-law dependence of the thermal conductivity on temperature is 0.81. The small deviation of the shock velocity from boundary-layer theory predicted by higher-order theory is not observed, though since both theories fall within the estimated experimental error this result is somewhat qualified. In any case, the unexpected agreement with first-order theory indicates that molecular effects, such as temperature jump, do not play a large role when the shock is more than ten shock thicknesses from the end wall.

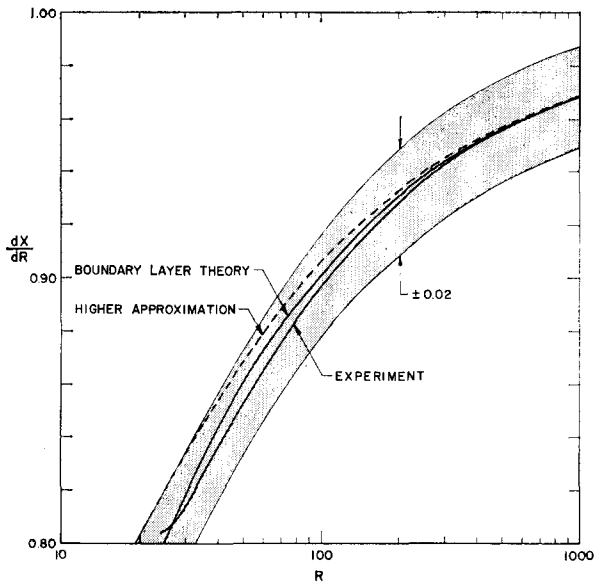

FIG. 7. Nondimensional shock velocity.

ACKNOWLEDGMENT

This work was supported by the National Aeronautics and Space Administration under Grant NsG-40-60.

[19] This comparison was suggested to us by Professor T. Kubota.